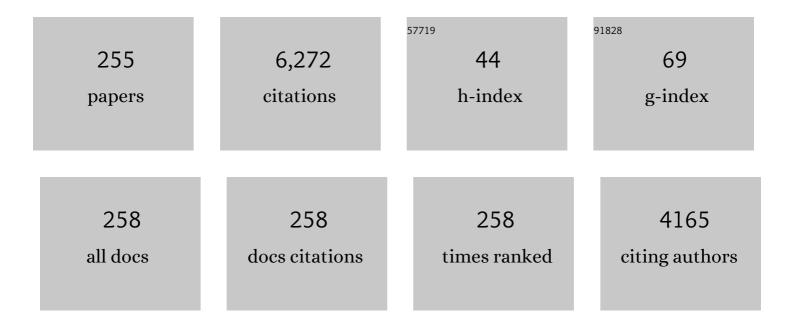
## Gaetano Scamarcio

List of Publications by Year in descending order

Source: https://exaly.com/author-pdf/7567991/publications.pdf Version: 2024-02-01



#	Article	IF	CITATIONS
1	Quartz-Enhanced Photoacoustic Spectroscopy: A Review. Sensors, 2014, 14, 6165-6206.	2.1	336
2	Single-molecule detection with a millimetre-sized transistor. Nature Communications, 2018, 9, 3223.	5.8	184
3	High-Power Infrared (8-Micrometer Wavelength) Superlattice Lasers. Science, 1997, 276, 773-776.	6.0	161
4	Part-per-trillion level SF_6 detection using a quartz enhanced photoacoustic spectroscopy-based sensor with single-mode fiber-coupled quantum cascade laser excitation. Optics Letters, 2012, 37, 4461.	1.7	142
5	Size-dependent lattice contraction inCdS1â^'xSexnanocrystals embedded in glass observed by Raman scattering. Physical Review B, 1992, 45, 13792-13795.	1.1	136
6	Size dependence of electron—LO-phonon coupling in semiconductor nanocrystals. Physical Review B, 1996, 53, R10489-R10492.	1.1	134
7	Measurement of subband electronic temperatures and population inversion in THz quantum-cascade lasers. Applied Physics Letters, 2005, 86, 111115.	1.5	123
8	Intracavity quartz-enhanced photoacoustic sensor. Applied Physics Letters, 2014, 104, .	1.5	115
9	Analysis of the electro-elastic properties of custom quartz tuning forks for optoacoustic gas sensing. Sensors and Actuators B: Chemical, 2016, 227, 539-546.	4.0	110
10	Interfacial electronic effects in functional biolayers integrated into organic field-effect transistors. Proceedings of the National Academy of Sciences of the United States of America, 2012, 109, 6429-6434.	3.3	109
11	Terahertz quartz enhanced photo-acoustic sensor. Applied Physics Letters, 2013, 103, .	1.5	107
12	Intrinsic stability of quantum cascade lasers against optical feedback. Optics Express, 2013, 21, 13748.	1.7	103
13	Ultimately Sensitive Organic Bioelectronic Transistor Sensors by Materials and Device Structure Design. Advanced Functional Materials, 2020, 30, 1904513.	7.8	97
14	Widely-tunable mid-infrared fiber-coupled quartz-enhanced photoacoustic sensor for environmental monitoring. Optics Express, 2014, 22, 28222.	1.7	93
15	Effect of interfacial bonding on the structural and vibrational properties of InAs/GaSb superlattices. Physical Review B, 1996, 53, 15688-15705.	1.1	86
16	About the amplification factors in organic bioelectronic sensors. Materials Horizons, 2020, 7, 999-1013.	6.4	86
17	First order Raman scattering in GaN. Solid State Communications, 1986, 58, 823-824.	0.9	83
18	Exciton localization in submonolayer InAs/GaAs multiple quantum wells. Physical Review B, 1990, 42, 3209-3212.	1.1	78

#	Article	IF	CITATIONS
19	A quartz enhanced photo-acoustic gas sensor based on a custom tuning fork and a terahertz quantum cascade laser. Analyst, The, 2014, 139, 2079-2087.	1.7	77
20	THz Quartz-enhanced photoacoustic sensor for H_2S trace gas detection. Optics Express, 2015, 23, 7574.	1.7	76
21	Thermal modeling of GalnAsâ^•AlInAs quantum cascade lasers. Journal of Applied Physics, 2006, 100, 043109.	1.1	73
22	Allan Deviation Plot as a Tool for Quartz-Enhanced Photoacoustic Sensors Noise Analysis. IEEE Transactions on Ultrasonics, Ferroelectrics, and Frequency Control, 2016, 63, 555-560.	1.7	72
23	Simultaneous measurement of the electronic and lattice temperatures in GaAs/Al0.45Ga0.55As quantum-cascade lasers: Influence on the optical performance. Applied Physics Letters, 2004, 84, 3690-3692.	1.5	70
24	Phase-resolved terahertz self-detection near-field microscopy. Optics Express, 2018, 26, 18423.	1.7	70
25	High-performance superlattice quantum cascade lasers. IEEE Journal of Selected Topics in Quantum Electronics, 1999, 5, 792-807.	1.9	69
26	Mid-infrared fiber-coupled QCL-QEPAS sensor. Applied Physics B: Lasers and Optics, 2013, 112, 25-33.	1.1	66
27	The double layer capacitance of ionic liquids for electrolyte gating of ZnO thin film transistors and effect of gate electrodes. Journal of Materials Chemistry C, 2017, 5, 3509-3518.	2.7	66
28	Selective single-molecule analytical detection of C-reactive protein in saliva with an organic transistor. Analytical and Bioanalytical Chemistry, 2019, 411, 4899-4908.	1.9	66
29	High-power inter-miniband lasing in intrinsic superlattices. Applied Physics Letters, 1998, 72, 2388-2390.	1.5	64
30	Label-Free and Selective Single-Molecule Bioelectronic Sensing with a Millimeter-Wide Self-Assembled Monolayer of Anti-Immunoglobulins. Chemistry of Materials, 2019, 31, 6476-6483.	3.2	62
31	Electrosynthesis and analytical characterisation of polypyrrole thin films modified with copper nanoparticles. Journal of Materials Chemistry, 2001, 11, 1434-1440.	6.7	61
32	Quartz-enhanced photoacoustic spectroscopy exploiting tuning fork overtone modes. Applied Physics Letters, 2015, 107, .	1.5	61
33	Terahertz quantum cascade lasers with large wall-plug efficiency. Applied Physics Letters, 2007, 90, 191115.	1.5	60
34	Improved Tuning Fork for Terahertz Quartz-Enhanced Photoacoustic Spectroscopy. Sensors, 2016, 16, 439.	2.1	59
35	Organic Field-Effect Transistor Platform for Label-Free, Single-Molecule Detection of Genomic Biomarkers. ACS Sensors, 2020, 5, 1822-1830.	4.0	59
36	Temperature profile of GaInAs/AlInAs/InP quantum cascade-laser facets measured by microprobe photoluminescence. Applied Physics Letters, 2001, 78, 2095-2097.	1.5	58

#	Article	IF	CITATIONS
37	Optical Anisotropy in Single Light-Emitting Polymer Nanofibers. Journal of Physical Chemistry C, 2011, 115, 20399-20405.	1.5	58
38	Highly sensitive gas leak detector based on a quartz-enhanced photoacoustic SF6 sensor. Optics Express, 2016, 24, 15872.	1.7	57
39	Standalone operation of an ECOFET for ultra-sensitive detection of HIV. Biosensors and Bioelectronics, 2020, 156, 112103.	5.3	57
40	Temperature Dependence of Thermal Conductivity and Boundary Resistance in THz Quantum Cascade Lasers. IEEE Journal of Selected Topics in Quantum Electronics, 2008, 14, 431-435.	1.9	52
41	Characterization of Covalently Bound Antiâ€Human Immunoglobulins on Selfâ€Assembled Monolayer Modified Gold Electrodes. Advanced Biology, 2017, 1, e1700055.	3.0	51
42	Reliability of visible GaN LEDs in plastic package. Microelectronics Reliability, 2003, 43, 1737-1742.	0.9	50
43	Thermal properties of THz quantum cascade lasers based on different optical waveguide configurations. Applied Physics Letters, 2006, 89, 021111.	1.5	46
44	High-resolution monitoring of the hole depth during ultrafast laser ablation drilling by diode laser self-mixing interferometry. Optics Letters, 2011, 36, 822.	1.7	45
45	Comparative analysis of resonant phonon THz quantum cascade lasers. Journal of Applied Physics, 2007, 101, 086109.	1.1	44
46	Influence of InAs, AlAs δ layers on the optical, electronic, and thermal characteristics of strain-compensated GalnAsâ`•AlInAs quantum-cascade lasers. Applied Physics Letters, 2007, 91, .	1.5	43
47	Large-Area Interfaces for Single-Molecule Label-free Bioelectronic Detection. Chemical Reviews, 2022, 122, 4636-4699.	23.0	43
48	Low-Loss Hollow Waveguide Fibers for Mid-Infrared Quantum Cascade Laser Sensing Applications. Sensors, 2013, 13, 1329-1340.	2.1	42
49	Ultra-low HIV-1 p24 detection limits with a bioelectronic sensor. Analytical and Bioanalytical Chemistry, 2020, 412, 811-818.	1.9	42
50	UV crosslinked poly(acrylic acid): a simple method to bio-functionalize electrolyte-gated OFET biosensors. Journal of Materials Chemistry B, 2015, 3, 5049-5057.	2.9	41
51	High finesse optical cavity coupled with a quartz-enhanced photoacoustic spectroscopic sensor. Analyst, The, 2015, 140, 736-743.	1.7	41
52	Large area laser-induced periodic surface structures on steel by bursts of femtosecond pulses with picosecond delays. Optics and Lasers in Engineering, 2019, 114, 15-21.	2.0	39
53	Infrared reflectivity by transverse-optical phonons in (GaAs)m/(AlAs)nultrathin-layer superlattices. Physical Review B, 1991, 43, 14754-14757.	1.1	38
54	Synthesis and optical investigations of low molecular weight alkoxy-substituted poly(p-phenylenevinylene)s. Journal of Materials Chemistry, 2000, 10, 1573-1579.	6.7	38

#	Article	IF	CITATIONS
55	Electron-lattice coupling in bound-to-continuum THz quantum-cascade lasers. Applied Physics Letters, 2006, 88, 241109.	1.5	38
56	Thermal Modeling of Terahertz Quantum-Cascade Lasers: Comparison of Optical Waveguides. IEEE Journal of Quantum Electronics, 2008, 44, 680-685.	1.0	38
57	Imaging of free carriers in semiconductors via optical feedback in terahertz quantum cascade lasers. Applied Physics Letters, 2014, 104, .	1.5	37
58	A quartz-enhanced photoacoustic sensor for H2S trace-gas detection at 2.6Âμm. Applied Physics B: Lasers and Optics, 2015, 119, 21-27.	1.1	37
59	Quantum Cascade Laser-Based Photoacoustic Sensor for Trace Detection of Formaldehyde Gas. Sensors, 2009, 9, 2697-2705.	2.1	36
60	Mapping propagation of collective modes in Bi2Se3 and Bi2Te2.2Se0.8 topological insulators by near-field terahertz nanoscopy. Nature Communications, 2021, 12, 6672.	5.8	36
61	Micro-Raman scattering in ultrathin-layer superlattices: Evidence of zone-center anisotropy of optical phonons. Physical Review B, 1993, 47, 1483-1488.	1.1	35
62	Improved thermal management of mid-IR quantum cascade lasers. Journal of Applied Physics, 2008, 103, .	1.1	35
63	Laserâ€5elfâ€Mixing Interferometry for Mechatronics Applications. Sensors, 2009, 9, 3527-3548.	2.1	35
64	Strong reduction of interchain interaction by bridged chain substitution in luminescent phenylenevinylene thin films. Applied Physics Letters, 1999, 75, 2053-2055.	1.5	34
65	Thermal resistance and temperature characteristics of GaAs/Al0.33Ga0.67As quantum-cascade lasers. Applied Physics Letters, 2001, 78, 1177-1179.	1.5	33
66	Printed, cost-effective and stable poly(3-hexylthiophene) electrolyte-gated field-effect transistors. Journal of Materials Chemistry C, 2020, 8, 15312-15321.	2.7	33
67	New trends in single-molecule bioanalytical detection. Analytical and Bioanalytical Chemistry, 2020, 412, 5005-5014.	1.9	33
68	Synthesis and characterization of poly(2,3,5,6-tetrafluoro-1,4-phenylenevinylene). Chemical Communications, 2001, , 1940-1941.	2.2	32
69	Subband electronic temperatures and electron-lattice energy relaxation in terahertz quantum cascade lasers with different conduction band offsets. Applied Physics Letters, 2006, 89, 131114.	1.5	32
70	Single mode operation with mid-IR hollow fibers in the range 51-105 µm. Optics Express, 2015, 23, 195.	1.7	32
71	A Comparative Study of the Gas Sensing Behavior in P3HT- and PBTTT-Based OTFTs: The Influence of Film Morphology and Contact Electrode Position. Sensors, 2014, 14, 16869-16880.	2.1	31
72	In Vitro Assessment of the Antibacterial Potential of Silver Nano-Coatings on Cotton Gauzes for Prevention of Wound Infections. Materials, 2016, 9, 411.	1.3	31

#	Article	IF	CITATIONS
73	Tunable, Gratingâ€Gated, Grapheneâ€Onâ€Polyimide Terahertz Modulators. Advanced Functional Materials, 2021, 31, 2008039.	7.8	31
74	Degradation mechanisms of GaN-based LEDs after accelerated DC current aging. , 0, , .		30
75	Simultaneous measurement of multiple target displacements by self-mixing interferometry in a single laser diode. Optics Express, 2011, 19, 16160.	1.7	30
76	A Compact Three Degrees-of-Freedom Motion Sensor Based on the Laser-Self-Mixing Effect. IEEE Photonics Technology Letters, 2008, 20, 1360-1362.	1.3	29
77	A Study on the Stability of Water-Gated Organic Field-Effect-Transistors Based on a Commercial p-Type Polymer. Frontiers in Chemistry, 2019, 7, 667.	1.8	29
78	Tunable interminiband infrared emission in superlattice electron transport. Applied Physics Letters, 1997, 70, 1796-1798.	1.5	28
79	Photoacoustic Spectroscopy with Quantum Cascade Lasers for Trace Gas Detection. Sensors, 2006, 6, 1411-1419.	2.1	28
80	Time-resolved measurement of the local lattice temperature in terahertz quantum cascade lasers. Applied Physics Letters, 2008, 92, 101116.	1.5	28
81	Raman scattering in CdTe1-xSex and CdS1-xSex nanocrystals embedded in glass. Superlattices and Microstructures, 1994, 16, 51-54.	1.4	27
82	Electronic distribution in superlattice quantum cascade lasers. Applied Physics Letters, 2000, 77, 1088-1090.	1.5	27
83	Coupling external cavity mid-IR quantum cascade lasers with low loss hollow metallic/dielectric waveguides. Applied Physics B: Lasers and Optics, 2012, 108, 255-260.	1.1	27
84	QCL-based nonlinear sensing of independent targets dynamics. Optics Express, 2014, 22, 5867.	1.7	26
85	Nonequilibrium optical phonon generation by steady-state electron transport in quantum-cascade lasers. Applied Physics Letters, 2002, 80, 4303-4305.	1.5	25
86	Nanoscale heat transfer in quantum cascade lasers. Physica E: Low-Dimensional Systems and Nanostructures, 2008, 40, 1780-1784.	1.3	25
87	Optical and Electronic NOx Sensors for Applications in Mechatronics. Sensors, 2009, 9, 3337-3356.	2.1	25
88	Experimental investigation of the lattice and electronic temperatures in Ga0.47In0.53Asâ^•Al0.62Ga0.38As1â^'xSbx quantum-cascade lasers. Applied Physics Letters, 2007, 90, 121109.	1.5	24
89	Non-equilibrium longitudinal and transverse optical phonons in terahertz quantum cascade lasers. Applied Physics Letters, 2012, 100, .	1.5	24
90	Continuous-Wave Reflection Imaging Using Optical Feedback Interferometry in Terahertz and Mid-Infrared Quantum Cascade Lasers. IEEE Transactions on Terahertz Science and Technology, 2014, 4, 631-633.	2.0	23

#	Article	IF	CITATIONS
91	Photo-generated metamaterials induce modulation of CW terahertz quantum cascade lasers. Scientific Reports, 2015, 5, 16207.	1.6	23
92	Terahertz near-field nanoscopy based on detectorless laser feedback interferometry under different feedback regimes. APL Photonics, 2021, 6, .	3.0	23
93	Thermal characteristics of quantum-cascade lasers by micro-probe optical spectroscopy. IEE Proceedings: Optoelectronics, 2003, 150, 298.	0.8	22
94	Impact of nonequilibrium phonons on the electron dynamics in terahertz quantum cascade lasers. Applied Physics Letters, 2010, 97, .	1.5	22
95	Enhancing the Sensitivity of Biotinylated Surfaces by Tailoring the Design of the Mixed Self-Assembled Monolayer Synthesis. ACS Omega, 2020, 5, 16762-16771.	1.6	22
96	Long-wavelength interminiband Fabry-Pérot and distributed feedback quantum cascade lasers. Semiconductor Science and Technology, 1998, 13, 1333-1339.	1.0	21
97	Probing quantum efficiency by laser-induced hot-electron cooling. Applied Physics Letters, 2009, 94, 021115.	1.5	21
98	Low-Loss Coupling of Quantum Cascade Lasers into Hollow-Core Waveguides with Single-Mode Output in the 3.7–7.6 μm Spectral Range. Sensors, 2016, 16, 533.	2.1	21
99	Structural and vibrational properties of (InAs)m(GaAs)nstrained superlattices grown by molecular beam epitaxy. Journal of Applied Physics, 1991, 69, 786-792.	1.1	20
100	Electronic Transduction of Proton Translocations in Nanoassembled Lamellae of Bacteriorhodopsin. ACS Nano, 2014, 8, 7834-7845.	7.3	20
101	Optical properties of highly excited ZnSe/ZnSxSe1-xmultiple-quantum-well structures. Semiconductor Science and Technology, 1992, 7, 681-685.	1.0	19
102	Laser-self-mixing interferometry in the Gaussian beam approximation: experiments and theory. Optics Express, 2010, 18, 10323.	1.7	19
103	Linewidth measurement of mid infrared quantum cascade laser by optical feedback interferometry. Applied Physics Letters, 2016, 108, .	1.5	19
104	Real time ablation rate measurement during high aspect-ratio hole drilling with a 120-ps fiber laser. Optics Express, 2012, 20, 663.	1.7	18
105	Detection of ultrafast laser ablation using quantum cascade laser-based sensing. Applied Physics Letters, 2012, 101, .	1.5	18
106	Effect of the gate metal work function on water-gated ZnO thin-film transistor performance. Journal Physics D: Applied Physics, 2016, 49, 275101.	1.3	18
107	Radiative decay of excitonic states in bulklike GaAs with a periodic array of InAs lattice planes. Physical Review B, 1990, 42, 11396-11399.	1.1	17
108	Interface characterization of InAs/AISb heterostructures by far infrared optical spectroscopy. Applied Physics Letters, 1994, 65, 2060-2062.	1.5	17

#	Article	IF	CITATIONS
109	High peak power (2.2 W) superlattice quantum cascade laser. Electronics Letters, 2001, 37, 295.	0.5	17
110	Influence of the band-offset on the electronic temperature of GaAs/Al(Ga)As superlattice quantum cascade lasers. Semiconductor Science and Technology, 2004, 19, S110-S112.	1.0	17
111	Simultaneous measurement of linear and transverse displacements by laser self-mixing. Applied Optics, 2009, 48, 1784.	2.1	17
112	Laser-Self-Mixing Fiber Sensor for Integral Strain Measurement. Journal of Lightwave Technology, 2011, 29, 335-340.	2.7	17
113	Volatile general anesthetic sensing with organic field-effect transistors integrating phospholipid membranes. Biosensors and Bioelectronics, 2013, 40, 303-307.	5.3	17
114	Nanoscale Displacement Sensing Based on Nonlinear Frequency Mixing in Quantum Cascade Lasers. IEEE Journal of Selected Topics in Quantum Electronics, 2015, 21, 107-114.	1.9	16
115	Why a Diffusing Singleâ€Molecule can be Detected in Few Minutes by a Large Capturing Bioelectronic Interface. Advanced Science, 2022, 9, e2104381.	5.6	16
116	Experimental determination of the temperature distribution in trench-confined oxide vertical-cavity surface-emitting lasers. IEEE Journal of Quantum Electronics, 2003, 39, 701-707.	1.0	15
117	Thermoelastic stress in GaAs/AlGaAs quantum cascade lasers. Applied Physics Letters, 2003, 82, 4639-4641.	1.5	15
118	Templateless synthesis of polypyrrole nanowires by non-static solution-surface electropolymerization. Journal of Solid State Electrochemistry, 2016, 20, 2143-2151.	1.2	15
119	Structural and Morphological Study of a Poly(3-hexylthiophene)/Streptavidin Multilayer Structure Serving as Active Layer in Ultra-Sensitive OFET Biosensors. Journal of Physical Chemistry C, 2014, 118, 15853-15862.	1.5	14
120	Phonons in Si/GaAs superlattices. Physical Review B, 1992, 46, 7296-7299.	1.1	13
121	Midinfrared emission from coupled Wannier-Stark ladders in semiconductor superlattices. Physical Review B, 1998, 57, R6811-R6814.	1.1	13
122	Si-GaAs(001) superlattice structure. Journal of Crystal Growth, 1993, 127, 121-125.	0.7	12
123	Narrowâ€band electroluminescence at 3.5 μm from impact excitation and ionization of Fe2+ ions in InP. Applied Physics Letters, 1996, 68, 1374-1376.	1.5	12
124	High Fe2+/3+ trap concentration in heavily compensated implanted InP. Applied Physics A: Materials Science and Processing, 2001, 73, 35-38.	1.1	12
125	High degradation and no bioavailability of artichoke miRNAs assessed using an in vitro digestion/Caco-2 cell model. Nutrition Research, 2018, 60, 68-76.	1.3	12
126	Monte Carlo simulation of tunable mid-infrared emission from coupled Wannier–Stark ladders in semiconductor superlattices. Applied Physics Letters, 2003, 82, 4029-4031.	1.5	11

#	Article	IF	CITATIONS
127	A large-area organic transistor with 3D-printed sensing gate for noninvasive single-molecule detection of pancreatic mucinous cyst markers. Analytical and Bioanalytical Chemistry, 2022, 414, 5657-5669.	1.9	11
128	Dependence of ?Reststrahlen? bands in far-infrared reflectivity on configuration of GaAs/AlAs multiple quantum well heterostructures. Applied Physics A: Solids and Surfaces, 1990, 51, 252-254.	1.4	10
129	Anisotropic heat propagation velocity in quantum cascade lasers. Applied Physics Letters, 2010, 96, 101101.	1.5	9
130	Self-mixing in multi-transverse mode semiconductor lasers: model and potential application to multi-parametric sensing. Optics Express, 2012, 20, 6286.	1.7	9
131	Versatile Multimodality Imaging System Based on Detectorless and Scanless Optical Feedback Interferometry—A Retrospective Overview for A Prospective Vision. Sensors, 2020, 20, 5930.	2.1	9
132	Hot-phonon generation in THz quantum cascade lasers. Journal of Physics: Conference Series, 2007, 92, 012018.	0.3	8
133	Laser ablation dynamics in metals: The thermal regime. Applied Physics Letters, 2012, 101, .	1.5	8
134	Electronic temperatures of terahertz quantum cascade active regions with phonon scattering assisted injection and extraction scheme. Optics Express, 2013, 21, 10172.	1.7	8
135	Bio-functionalization of ZnO water gated thin-film transistors. , 2015, , .		8
136	Spectroscopy study of monolayer InAs/GaAs single and multiple quantum wells grown by molecular beam epitaxy. Superlattices and Microstructures, 1991, 9, 147-150.	1.4	7
137	Hot Electrons in THz Quantum Cascade Lasers. Journal of Infrared, Millimeter, and Terahertz Waves, 2013, 34, 357-373.	1.2	7
138	Surface composition of mixed self-assembled monolayers on Au by infrared attenuated total reflection spectroscopy. Applied Surface Science, 2021, 559, 149883.	3.1	7
139	Deep-level electroluminescence at 3.5 µm from semi-insulating InP layers ion implanted with Fe. Semiconductor Science and Technology, 2001, 16, L1-L3.	1.0	6
140	Quantum cascade laser-based photoacoustic spectroscopy of volatile chemicals: Application to hexamethyldisilazane. Spectrochimica Acta - Part A: Molecular and Biomolecular Spectroscopy, 2006, 64, 426-429.	2.0	6
141	On Line Sensing of Ultrafast Laser Microdrilling Processes by Optical Feedback Interferometry. Physics Procedia, 2013, 41, 670-676.	1.2	6
142	Wide wavelength tuning of GaAsâ^•AlxGa1â^'xAs bound-to-continuum quantum cascade lasers by aluminum content control. Applied Physics Letters, 2008, 92, .	1.5	5
143	Trace gas sensing using quantum cascade lasers and a fiber-coupled optoacoustic sensor: Application to formaldehyde. Journal of Physics: Conference Series, 2010, 214, 012037.	0.3	5
144	Electrochemical deposition of gold on indium zirconate (InZrOx with In/Zr atomic ratio 1.0) for high temperature automobile exhaust gas sensors. Journal of Solid State Electrochemistry, 2015, 19, 2859-2868.	1.2	5

#	Article	IF	CITATIONS
145	Negatively charged ions to probe self-assembled monolayer reorganization driven by interchain interactions. Journal of Materials Chemistry C, 2021, 9, 10935-10943.	2.7	5
146	Infrared reflectivity of strained GaSb/AlSb superlattices. Solid-State Electronics, 1994, 37, 625-628.	0.8	4
147	Facet temperature mapping of GaAs/AlGaAs quantum cascade lasers by photoluminescence microprobe. Optical Materials, 2001, 17, 219-222.	1.7	4
148	Direct measurement of the local temperature distribution in oxide VCSELs. , 2002, , .		4
149	Implant and characterization of highly concentrated Fe deep centers in InP. Materials Science and Engineering B: Solid-State Materials for Advanced Technology, 2002, 91-92, 503-507.	1.7	4
150	Optical far-IR wave generation - state-of-the-art and advanced device structures. , 2004, , .		4
151	Functionalized interfaces by plasma treatments on silicon and silicon dioxide substrates. Thin Solid Films, 2007, 515, 7195-7202.	0.8	4
152	Au/In <sub>2</sub> O <sub>3</sub> and Au/ZrO <sub>2</sub> composite nanoparticles via <i>in situ</i> sacrificial gold electrolysis. Materials Express, 2015, 5, 171-179.	0.2	4
153	Determination of superlattice structural parameters by means of far- and mid-infrared reflectivity. Solid State Communications, 1992, 84, 757-760.	0.9	3
154	Radiative recombination processes in ZnSe/ZnSexSe1â^'x multiple-quantum-well structures. Physica B: Condensed Matter, 1993, 185, 352-356.	1.3	3
155	Assessment of interface composition in superlattices by far-infrared reflectivity. Physical Review B, 1994, 49, 2604-2607.	1.1	3
156	Evidence of electronic confinement in pseudomorphic Si/GaAs superlattices. Physical Review B, 1998, 57, R15100-R15103.	1.1	3
157	Assessment of electrical and optical properties of heavily Fe-implanted semi-insulating InP. Materials Science and Engineering B: Solid-State Materials for Advanced Technology, 2001, 80, 202-205.	1.7	3
158	Widely tunable mid-infrared emission from coupled Wannier–Stark ladders in semiconductor superlattices. Physica B: Condensed Matter, 2002, 314, 332-335.	1.3	3
159	<title>Nondestructive technique for the direct measurement of the local temperature distribution in VCSELs</title> . , 2002, 4648, 22.		3
160	Non equilibrium electrons in THz quantum cascade lasers. , 2006, 6133, 126.		3
161	Mid-IR quantum cascade laser mode coupling in hollow-core, fiber-optic waveguides with single-mode beam delivery. Proceedings of SPIE, 2015, , .	0.8	3
162	Improved Performance p-type Polymer (P3HT) / n-type Nanotubes (WS2) Electrolyte Gated Thin-Film Transistor. MRS Advances, 2018, 3, 1525-1533.	0.5	3

#	Article	IF	CITATIONS
163	A label-free immunosensor based on a graphene water-gated field-effect transistor. , 2019, , .		3
164	Infrared reflectivity and Raman spectra of (GaAs)m(AlAs)n ultrathin layer superlattices. Surface Science, 1992, 267, 430-433.	0.8	2
165	Influence of the interface bond type on the farâ€infrared reflectivity of InAs/GaSb superlattices. Journal of Applied Physics, 1995, 78, 5642-5644.	1.1	2
166	Three-terminal mid-IR tunable emitters based on Wannier–Stark ladder transitions in semiconductor superlattices. Semiconductor Science and Technology, 2004, 19, S87-S88.	1.0	2
167	Comparison of plane mirror vs retroreflector performance for laser-self-mixing displacement sensors. Journal of the European Optical Society-Rapid Publications, 0, 4, .	0.9	2
168	Hot electron effects and nanoscale heat transfer in Terahertz quantum cascade lasers. Proceedings of SPIE, 2009, , .	0.8	2
169	Heat transport in terahertz quantum cascade lasers. Optical Engineering, 2010, 49, 111115.	0.5	2
170	Direct investigation of the ablation rate evolution during laser drilling of high aspect ratio micro-holes. Proceedings of SPIE, 2012, , .	0.8	2
171	THz quartz-enhanced photoacoustic sensor employing a quantum cascade laser source. Proceedings of SPIE, 2013, , .	0.8	2
172	New approaches in quartz-enhanced photoacoustic sensing. Proceedings of SPIE, 2015, , .	0.8	2
173	Innovative quartz enhanced photoacoustic sensors for trace gas detection. , 2016, , .		2
174	Electrolyte gated TFT biosensors based on the Donnan's capacitance of anchored biomolecules. , 2017, , .		2
175	One- and two-phonon scattering processes in ZnSe/ZnSxSe1â^'xsuperlattices studied by micro-Raman spectroscopy. Physical Review B, 1994, 50, 4988-4991.	1.1	1
176	Quantum-well-laser mirror degradation investigated by microprobe optical spectroscopy. , 1995, , .		1
177	Hot electron distribution in quantum cascade and single stage GaAs/AlGaAs periodic superlattice structures. Optical Materials, 2001, 17, 223-225.	1.7	1
178	High Fe solubility in InP by high temperature ion implantation. Nuclear Instruments & Methods in Physics Research B, 2001, 178, 275-278.	0.6	1
179	2-D temperature mapping of vertical-cavity surface-emitting lasers determined by microprobe electroluminescence. IEEE Photonics Technology Letters, 2002, 14, 266-268.	1.3	1
180	Electronic spatial distribution of In0.53Ga0.47Asâ^•AlAs0.56Sb0.44 quantum-cascade lasers. Journal of Applied Physics, 2005, 98, 086106.	1.1	1

#	Article	IF	CITATIONS
181	Electronic and lattice temperatures in bound-to-continuum terahertz quantum cascade lasers. , 2006, , .		1
182	Electronic and thermal properties of Sb-based QCLs operating in the first atmospheric window. , 2007, , $\cdot$		1
183	Plasma treatment effects on Si and Si/dielectric film heterostructures. Journal of Materials Processing Technology, 2008, 206, 462-466.	3.1	1
184	A no-contact laser sensor based on the Self-Mixing effect for the measurement of rotations. , 2008, , .		1
185	Microprobe photoluminescence assessment of the wall-plug efficiency in interband cascade lasers. Journal of Applied Physics, 2008, 104, 046101.	1.1	1
186	Photoacoustic trace gas sensing with mid-IR quantum cascade lasers. , 2009, , .		1
187	A self-mixing laser sensor for the real-time correction of straightness/flatness deviations of a linear slide. Proceedings of SPIE, 2009, , .	0.8	1
188	Laser-self-mixing interferometric fiber strain sensor. Proceedings of SPIE, 2009, , .	0.8	1
189	Monolithic focal plane arrays for terahertz active spectroscopic imaging: an experimental study. , 2011, , .		1
190	Cavity and quartz enhanced photo-acoustic mid-IR sensor. , 2013, , .		1
191	THz quantum cascade laser-based quartz enhanced photo-acoustic sensor. , 2013, , .		1
192	Coherent imaging with mid-IR and THz quantum cascade lasers through optical feedback interferometry. , 2013, , .		1
193	Carriers density imaging by self-mixing interferometry in a THz quantum cascade laser. , 2014, , .		1
194	Quantum cascade lasers with optical feedback: regular multimode dynamics. Proceedings of SPIE, 2015, , .	0.8	1
195	Quartz-enhanced photoacoustic sensors for H2S trace gas detection. , 2015, , .		1
196	New developments in THz quartz enhanced photoacoustic spectroscopy. , 2016, , .		1
197	Phase-resolved terahertz near-field nanoscopy of a topological insulator phonon-polariton mode. , 2018, , .		1
198	Effect of the ionic-strength of the gating-solution on a bioelectronic response. , 2019, , .		1

#	Article	IF	CITATIONS
199	Thermal Modelling of Quantum Cascade Lasers. Acta Physica Polonica A, 2009, 116, 451-454.	0.2	1
200	1-D and 2-D surface structuring of steel by bursts of femtosecond laser pulses. , 2019, , .		1
201	Mid-infrared (3.5 μm) electroluminescence from heavily Fe 2+ ion-implanted semi-insulating InP. Optical Materials, 2001, 17, 189-191.	1.7	0
202	State of the art of InP and GaAs quantum cascade lasers. , 0, , .		0
203	Hot electrons in resonant-phonon terahertz quantum cascade lasers. , 2005, , .		0
204	Electronic and Thermal properties of THz Quantum Cascade. , 2006, , .		0
205	Comparative Analysis of THz Quantum Cascade Lasers. , 2007, , .		0
206	Experimental measurement of the wall-plug efficiency in THz quantum cascade lasers. , 2007, , .		0
207	High performance THz quantum cascade laser with different optical waveguide configurations. , 2007,		0
208	Influence of substrate pre-treatments on the growth of SixNyHz thin films by plasma enhanced chemical vapor deposition. Surface and Coatings Technology, 2008, 202, 3081-3087.	2.2	0
209	All fiber strain sensor based on the Laser-Self-Mixing effect. , 2008, , .		0
210	Correlation between the subband electronic temperatures and the internal quantum efficiency of THz quantum cascade lasers. , 2008, , .		0
211	Heat transfer dynamics and temperature performance degradation in terahertz quantum cascade lasers. , 2009, , .		0
212	Time of flight measurements of the nanoscale heat transfer dynamic in terahertz quantum cascade lasers. , 2009, , .		0
213	All-interferometric six-degrees-of-freedom sensor based on laser self-mixing. , 2009, , .		0
214	Hot-electron cooling in THz quantum cascade lasers. , 2009, , .		0
215	Correlation between laser-induced hot-electron cooling and quantum efficiency in THz quantum cascade lasers. , 2009, , .		0
216	Trace gas sensing using quantum cascade lasers and optoacoustic detection. Proceedings of SPIE, 2009, , .	0.8	0

#	Article	IF	CITATIONS
217	Quantum-cascade-laser-based optoacoustic detection: application to nitric oxide and formaldehyde. Proceedings of SPIE, 2010, , .	0.8	Ο
218	Non-equilibrium LO and TO phonon generation by electron transport in Terahertz quantum cascade lasers. , 2010, , .		0
219	Perspectives in the design of monolithic focal plane arrays for terahertz active spectroscopic imaging. , 2010, , .		0
220	Advanced optoacoustic sensor designs for environmental applications. Proceedings of SPIE, 2010, , .	0.8	0
221	Heat transfer speed and phonon related phenomena in terahertz quantum cascade lasers. , 2010, , .		Ο
222	Core-shell gold nanoparticles and gold-decorated metal oxides for gas sensing applications. , 2011, , .		0
223	A new three degrees-of-freedom motion sensor based on laser-self-mixing with pigtailed sources. , 2011, , .		0
224	Laser self-mixing sensor to monitor in situ the penetration depth during short pulse laser drilling of metal targets. Proceedings of SPIE, 2011, , .	0.8	0
225	Innovative electronic biosensors based on organic thin film transistors. , 2011, , .		0
226	Real-time in-situ measurement of the penetration depth in short pulse laser percussion drilling of metal targets. , 2011, , .		0
227	Self-mixing in VCSELs for multi-parametric sensing applications: theory and experiment. Proceedings of SPIE, 2012, , .	0.8	0
228	Single QCL-based sensor measuring the simultaneous displacement of independent targets. Proceedings of SPIE, 2013, , .	0.8	0
229	Electronic temperature in phonon-photon-phonon terahertz quantum cascade devices with high-operating temperature performance. , 2013, , .		0
230	Part-per-trillion level detection of SF <sub>6</sub> using a single-mode fiber-coupled quantum cascade laser and a quartz enhanced photoacoustic sensor. Proceedings of SPIE, 2013, , .	0.8	0
231	Quantum cascade laser-based sensing to investigate fast laser ablation process. , 2013, , .		0
232	Measurement of relative velocity of independent targets by a quantum cascade laser subject to optical feedback. , 2014, , .		0
233	THz imaging of free carrier density based on quantum cascade lasers under optical feedback. , 2014, , .		0
234	Intracavity Quartz-Enhanced Photoacoustic Sensor for Mid-Infrared Trace-Gas Detection. , 2014, , .		0

#	Article	IF	CITATIONS
235	Nonlinear frequency mixing in QCL-based interferometry: beyond the intrinsic resolution. Proceedings of SPIE, 2015, , .	0.8	Ο
236	Linewidth measurement of a NIR VCSEL by self-mixing interferometry using voltage detection scheme. , 2016, , .		0
237	Linewidth Estimation Of A Mid Infrared Quantum Cascade Laser By Voltage Noise Spectral Density Measurement. , 2016, , .		0
238	Laser self-detection operation of a mid-IR near-field microscope. , 2016, , .		0
239	Hollow-core waveguide for single-mode laser beam propagation in the spectral range of 3.7-7.3 l̂¼m. , 2016, , .		0
240	Quartz enhanced photoacoustic leak sensor for mechatronic components. Proceedings of SPIE, 2016, ,	0.8	0
241	Quartz tuning forks with novel geometries for optoacoustic gas sensing. , 2016, , .		0
242	Characterization of modified working electrodes for sensing applications by means of electrolyte-gated TFT and cyclic voltammetry. , 2017, , .		0
243	Investigation and Modelling of Single-Molecule Organic Transistors. , 2019, , .		0
244	Analysis of Label-Free Single-Molecule Biosensors based on Gate-Biofunctionalized Organic Transistors. , 2019, , .		0
245	Terahertz Near-field Nanoscopy Based on Self-mixing Interferometry with Quantum Cascade Resonators. , 2021, , .		0
246	Experimental Investigation of Hot Carriers in THz and Mid-IR Quantum Cascade Lasers. Springer Proceedings in Physics, 2006, , 89-93.	0.1	0
247	Experimental Investigation of Hot Carriers in Terahertz Quantum Cascade Lasers. Acta Physica Polonica A, 2008, 113, 787-794.	0.2	0
248	Direct in-situ measurement of the ablation rate in short pulse laser percussion drilling of metal targets. , 2011, , .		0
249	Quartz Enhanced Photoacoustic Sensors for Trace Gas Detection in the IR and THz Spectral Range. NATO Science for Peace and Security Series B: Physics and Biophysics, 2014, , 139-151.	0.2	0
250	Raman Scattering in CdS1-x Se x Quantum Dots Embedded in Glass: Evidence of Size-Dependent Lattice Contraction. , 1993, , 393-401.		0
251	Radiative recombination processes in ZnSe/ZnSexSe1â^'x multiple-quantum-well structures. , 1993, , 352-356.		0
252	Sub-wavelength near field imaging techniques at terahertz frequencies. , 2018, , .		0

Sub-wavelength near field imaging techniques at terahertz frequencies. , 2018, , . 252

#	Article	IF	CITATIONS
253	Electron Transport in Novel Sb-based Quantum Cascade Lasers. , 2006, , 295-299.		Ο
254	Electrically Tunable Graphene-on-Polyimide Terahertz Modulators. , 2020, , .		0
255	Physical Modelling of Large-Area Single-Molecule Organic Transistors. , 2022, , .		0